Karlsruhe Institute of Technology

Vector-boson scattering - Impact of a concrete new-physics model versus its EFT realization

IMPRS EPP recruiting workshop

Jannis Lang in collaboration with Stefan Liebler, Heiko Schäfer-Siebert, Dieter Zeppenfeld | May 25, 2020

INSTITUTE FOR THEORETICAL PHYSICS

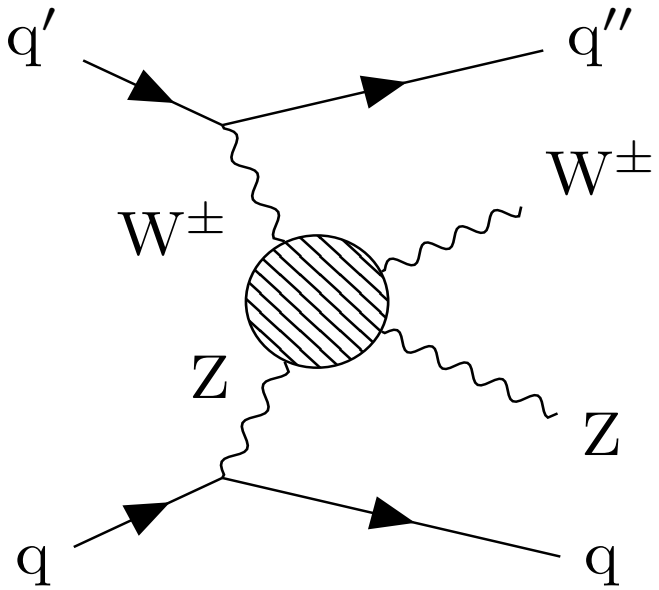

Outline

Overview

- New-physics (NP) contribution in Vector-boson scattering (VBS) described using effective field theory (EFT) operators (of dimension 8), e.g.

$$\mathrm{Tr}(\hat{W}^{\mu\nu}\hat{W}_{\mu\nu})\,\mathrm{Tr}(\hat{W}^{\alpha\beta}\hat{W}_{\alpha\beta}) \tag{1}$$

Historical examples:

Euler-Heisenberg Lagrangian:

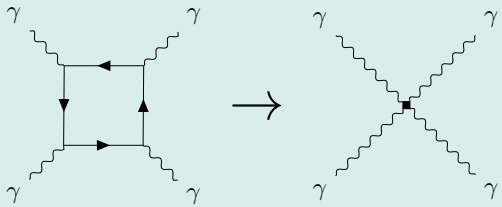

$$\rightarrow C_1 \cdot \left(F^{\mu\nu}F_{\mu\nu}\right)^2 + C_2 \cdot \left(F^{\mu\nu}\tilde{F}_{\mu\nu}\right)^2 \tag{2}$$

Effective Gluon-Gluon-Higgs Vertex:

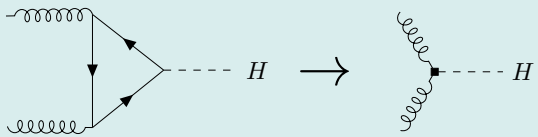

$$\rightarrow C \cdot \phi^\dagger \phi G^{\mu\nu} G_{\mu\nu} \tag{3}$$

EFT Basics

- Bottom up approach for model independent parametrization of NP
- Resulting Lagrangian by integrating out heavy fields

EFT expansion

$$\mathcal{L}_{eff} = \sum_{n=1}^{\infty} \sum_{i} \frac{f_i^{(n)}}{\Lambda^n} O_i^{(n+4)} \tag{4}$$

Λ energy scale of NP; f_i Wilson coefficient for operator O_i; $n+4$ energy dimension

$\Rightarrow$ Assumptions for our purpose:

- Underlying model affects $SU(2)_L$ gauge fields only
- No breaking of $SU(2)_L$ through NP

Constructing basis for EFT

- Convention: $\hat{W}_{\mu\nu} = \frac{1}{-ig}\left[\hat{D}_\mu, \hat{D}_\mu\right]$, $\hat{D}_\mu = \partial_\mu - ig\frac{\sigma^a}{2}W^a_\mu$

Dimension 6 operators

[Hagiwara, K. and Ishihara, S. and Szalapski, R. and Zeppenfeld, D. (1993); Phys. Rev. D 48, 2182]

$$O_{WWW} = \mathrm{Tr}\left(\hat{W}^{\mu}{}_{\nu}\,\hat{W}^{\nu}{}_{\rho}\,\hat{W}^{\rho}{}_{\mu}\right) \tag{5}$$

$$O_{DW} = \mathrm{Tr}\left([\hat{D}_\alpha, \hat{W}^{\mu\nu}][\hat{D}^\alpha, \hat{W}_{\mu\nu}]\right) \tag{6}$$

Transverse (T) operators

[O.J.P. Eboli, M.C. Gonzalez-Garcia, J.K. Mizukoshi (2006); arXiv:hep-ph/0606118]

$$O_{T,0} = \mathrm{Tr}\left(\hat{W}^{\mu\nu}\hat{W}_{\mu\nu}\right)\mathrm{Tr}\left(\hat{W}^{\alpha\beta}\hat{W}_{\alpha\beta}\right) \tag{7}$$

$$O_{T,1} = \mathrm{Tr}\left(\hat{W}^{\mu\nu}\hat{W}_{\alpha\beta}\right)\mathrm{Tr}\left(\hat{W}^{\alpha\beta}\hat{W}_{\mu\nu}\right) \tag{8}$$

$$O_{T,2} = \mathrm{Tr}\left(\hat{W}^{\mu\nu}\hat{W}_{\nu\alpha}\right)\mathrm{Tr}\left(\hat{W}^{\alpha\beta}\hat{W}_{\beta\mu}\right) \tag{9}$$

$$O_{T,3} = \mathrm{Tr}\left(\hat{W}^{\mu\nu}\hat{W}^{\alpha\beta}\right)\mathrm{Tr}\left(\hat{W}_{\nu\alpha}\hat{W}_{\beta\mu}\right) \tag{10}$$

DmWn operators used in our basis

$$O_{DWWW,0} = \mathrm{Tr}\left([\hat{D}_\alpha, \hat{W}^{\mu}{}_{\nu}][\hat{D}^\alpha, \hat{W}^{\nu}{}_{\rho}]\hat{W}^{\rho}{}_{\mu}\right) \tag{11}$$

$$O_{DWWW,1} = \mathrm{Tr}\left([\hat{D}_\alpha, \hat{W}^{\mu\nu}][\hat{D}_\beta, \hat{W}_{\mu\nu}]\hat{W}^{\alpha\beta}\right) \tag{12}$$

$$O_{D2W} = \mathrm{Tr}\left([\hat{D}_\alpha, [\hat{D}^\alpha, \hat{W}^{\mu\nu}]][\hat{D}_\beta, [\hat{D}^\beta, \hat{W}_{\mu\nu}]]\right) \tag{13}$$

Constructing basis for EFT

Full set of operators up to dimension 8

$$
\begin{aligned}
\mathcal{L}_{eff} = &\Big(f_{WW}\,\mathrm{Tr}\big(\hat{W}^{\mu\nu}\hat{W}_{\mu\nu}\big)\Big) + \frac{f_{DW}}{\Lambda^2}\,\mathrm{Tr}\big([\hat{D}_\alpha,\hat{W}^{\mu\nu}][\hat{D}^\alpha,\hat{W}_{\mu\nu}]\big) + \frac{f_{WWW}}{\Lambda^2}\,\mathrm{Tr}\big(\hat{W}^{\mu}{}_{\nu}\hat{W}^{\nu}{}_{\rho}\hat{W}^{\rho}{}_{\mu}\big) \\
&+ \frac{f_{D2W}}{\Lambda^4}\,\mathrm{Tr}\big([\hat{D}_\alpha,[\hat{D}^\alpha,\hat{W}^{\mu\nu}]][\hat{D}_\beta,[\hat{D}^\beta,\hat{W}_{\mu\nu}]]\big) + \frac{f_{DWWW,0}}{\Lambda^4}\,\mathrm{Tr}\big([\hat{D}_\alpha,\hat{W}^{\mu}{}_{\nu}][\hat{D}^\alpha,\hat{W}^{\nu}{}_{\rho}]\hat{W}^{\rho}{}_{\mu}\big) \\
&+ \frac{f_{DWWW,1}}{\Lambda^4}\,\mathrm{Tr}\big([\hat{D}_\alpha,\hat{W}^{\mu\nu}][\hat{D}_\beta,\hat{W}^{\mu\nu}]\hat{W}^{\alpha\beta}\big) \\
&+ \frac{f_{T,0}}{\Lambda^4}\,\mathrm{Tr}\big(\hat{W}^{\mu\nu}\hat{W}_{\mu\nu}\big)\,\mathrm{Tr}\big(\hat{W}^{\alpha\beta}\hat{W}_{\alpha\beta}\big) + \frac{f_{T,1}}{\Lambda^4}\,\mathrm{Tr}\big(\hat{W}^{\mu\nu}\hat{W}_{\alpha\beta}\big)\,\mathrm{Tr}\big(\hat{W}^{\alpha\beta}\hat{W}_{\mu\nu}\big) \\
&+ \frac{f_{T,2}}{\Lambda^4}\,\mathrm{Tr}\big(\hat{W}^{\mu}{}_{\nu}\hat{W}^{\nu}{}_{\alpha}\big)\,\mathrm{Tr}\big(\hat{W}^{\alpha}{}_{\beta}\hat{W}^{\beta}{}_{\mu}\big) + \frac{f_{T,3}}{\Lambda^4}\,\mathrm{Tr}\big(\hat{W}^{\mu\nu}\hat{W}^{\alpha\beta}\big)\,\mathrm{Tr}\big(\hat{W}_{\nu\alpha}\hat{W}_{\beta\mu}\big)
\end{aligned}
\tag{14}
$$

$\Rightarrow$ Feynman rules for EFT vertices

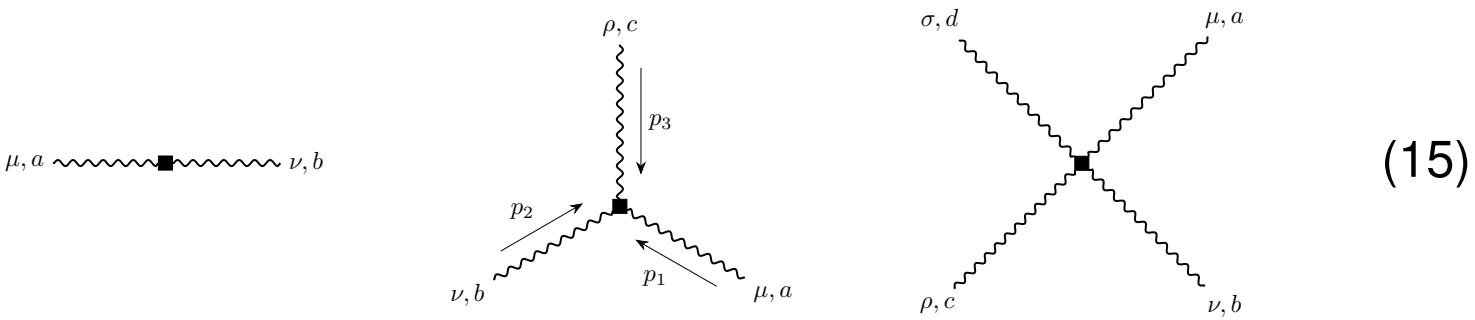

(15)

Lagrangian Density of NP model

- NP: fermion and scalar $SU(2)_L$ multiplets with mass $M_{F/S}$, isospin $J_{F/S}$ (well motivated through minimal dark matter models)
- Electroweak sector in $SU(2)_L$ limit of the Standard Model (SM):

$$g' \to 0 \Rightarrow m_W = m_Z; \quad Z = W^3; \quad \text{no } \gamma \tag{16}$$

- One-loop level only for NP contribution $\Rightarrow$ Unitary Gauge

Lagrangian

$$\mathcal{L} = \frac{1}{2}(\partial_\mu H)^2 - \frac{m_H^2}{2}H^2 - \frac{1}{2}\mathrm{Tr}\left(\hat{W}^{\mu\nu}\hat{W}_{\mu\nu}\right) + \frac{m_W^2}{2}\left(\sum_{a=1}^{3} W^a{}_\mu W^{a\mu}\right)\left(1+\frac{H}{v}\right)^2$$
$$+ \bar{\Psi}\left(i\gamma_\mu D^\mu - M_F\right)\Psi + \left(D^\mu\Phi\right)^\dagger D_\mu\Phi + {M_S}^2\Phi^\dagger\Phi\,, \tag{17}$$

with $D_\mu = \partial_\mu - igt^a_{F/S}W^a_\mu$

Calculate one-loop corrections

Representation factors

-  $\propto \mathrm{Tr}\left(t_F^a t_F^b\right) = T_F \delta^{ab}$
- 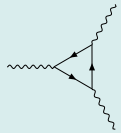 $\propto \mathrm{Tr}\left(t_F^a t_F^b t_F^c\right) = \frac{i}{2} T_F \epsilon^{abc}$
- 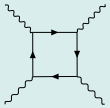 $\propto \mathrm{Tr}\left(t_F^a t_F^b t_F^d t_F^c\right) = \frac{1}{15} T_F (3C_{2,F} - 1)(\delta^{ab}\delta^{cd} + \delta^{ac}\delta^{bd} + \delta^{ad}\delta^{bc}) + \frac{1}{6} T_F (\delta^{ab}\delta^{cd} - 2\delta^{ac}\delta^{bd} + \delta^{ad}\delta^{bc})$

$$\Rightarrow SU(2): \quad C_{2,R} = J_R(J_R+1), \quad T_R = \frac{C_{2,R}\,dim(R)}{dim(A)} = \frac{J_R(J_R+1)(2J_R+1)}{3} \tag{18}$$

- W propagator correction:

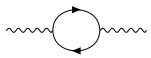 $= T_F\ \Pi_F^{\mu\nu}(p, M_F^2)\ \delta^{ab}$ (19)

- $3W$ vertex correction:

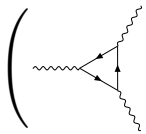 $+ \text{perm.}) = iT_F\ \Gamma_{3,F}^{\mu\nu\rho}(p_1, p_2, p_3, M_F^2)\ \epsilon^{abc}$ (20)

- $4W$ vertex correction:

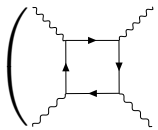 $+ \text{perm.}) = \Gamma_{4,F}^{\mu\nu\alpha\beta,abcd}(p_1, p_2, p_3, p_4, M_F^2, T_F, C_{2,F})$ (21)

Matching of Wilson Coefficients

- New physics scale $\Lambda \sim M_F, M_S$

$\Rightarrow$ Expand loop vertices in $\frac{p_i \cdot p_j}{M^2} \ll 1$ and match terms $\propto \frac{1}{M^2}$, $\propto \frac{1}{M^4}$ to terms $\propto \frac{1}{\Lambda^2}$, $\propto \frac{1}{\Lambda^4}$ in EFT Feynman rules, respectively

$$\frac{f_{T,0,F}}{\Lambda^4} = g^4 \frac{T_F}{10080\pi^2 M_F^4} \left(-14C_{2,F} + 1\right)$$
$$\frac{f_{T,1,F}}{\Lambda^4} = g^4 \frac{T_F}{10080\pi^2 M_F^4} \left(-28C_{2,F} + 13\right)$$
$$\frac{f_{T,2,F}}{\Lambda^4} = g^4 \frac{T_F}{25200\pi^2 M_F^4} \left(196C_{2,F} - 397\right)$$
$$\frac{f_{T,3,F}}{\Lambda^4} = g^4 \frac{T_F}{25200\pi^2 M_F^4} \left(98C_{2,F} + 299\right)$$

$$\frac{f_{T,0,S}}{\Lambda^4} = g^4 \frac{T_S}{40320\pi^2 M_S^4} \left(7C_{2,S} - 2\right)$$
$$\frac{f_{T,1,S}}{\Lambda^4} = g^4 \frac{T_S}{40320\pi^2 M_S^4} \left(14C_{2,S} - 5\right)$$
$$\frac{f_{T,2,S}}{\Lambda^4} = g^4 \frac{T_S}{50400\pi^2 M_S^4} \left(14C_{2,S} - 23\right)$$
$$\frac{f_{T,3,S}}{\Lambda^4} = g^4 \frac{T_S}{50400\pi^2 M_S^4} \left(7C_{2,S} + 16\right) \qquad (22)$$

Bounds on Wilson coefficients

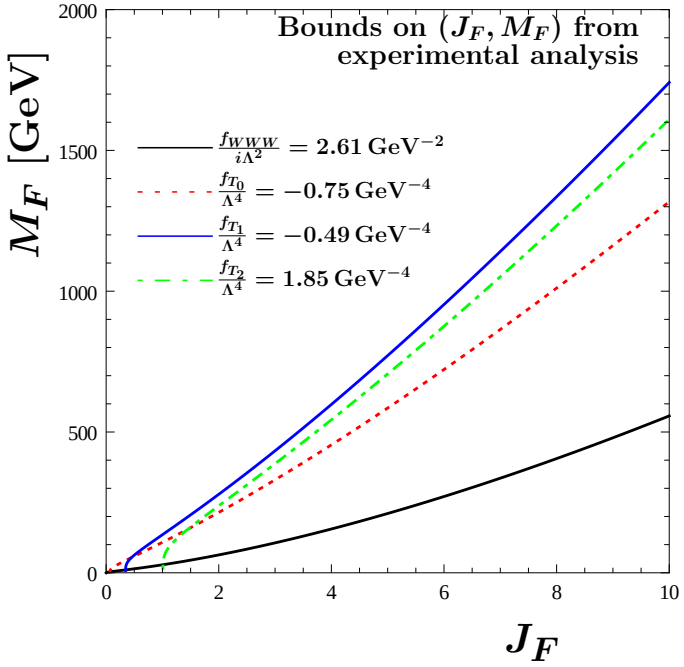

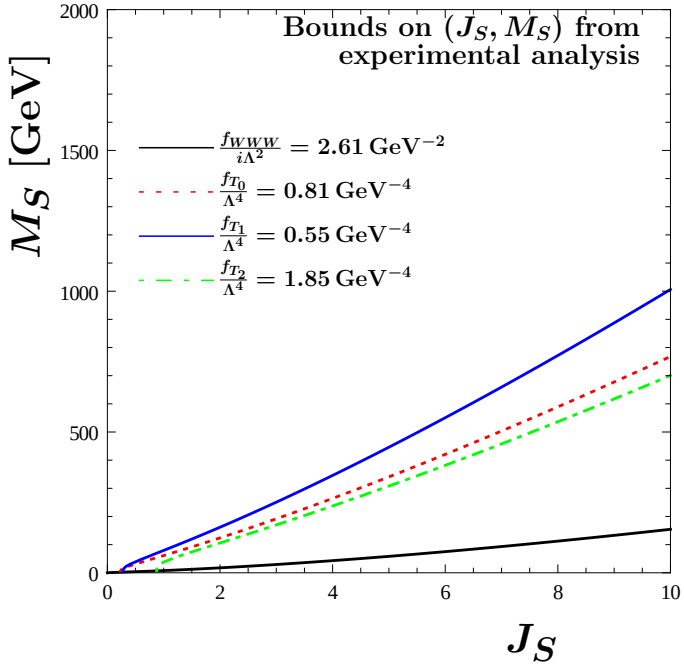

- Experimental bounds [PDG][Sirunyan et al. 2019, arXiv: 1901.04060 [hep-ex]] on anomalous couplings restrict parameter space

$\Rightarrow$ Strategy: Analyse model behaviour close to existing bounds, eg. ($M_F = 750\,\mathrm{GeV}$, $J_F = 5$) or ($M_S = 750\,\mathrm{GeV}$, $J_S = 8$)

Definitions for on-shell VBS

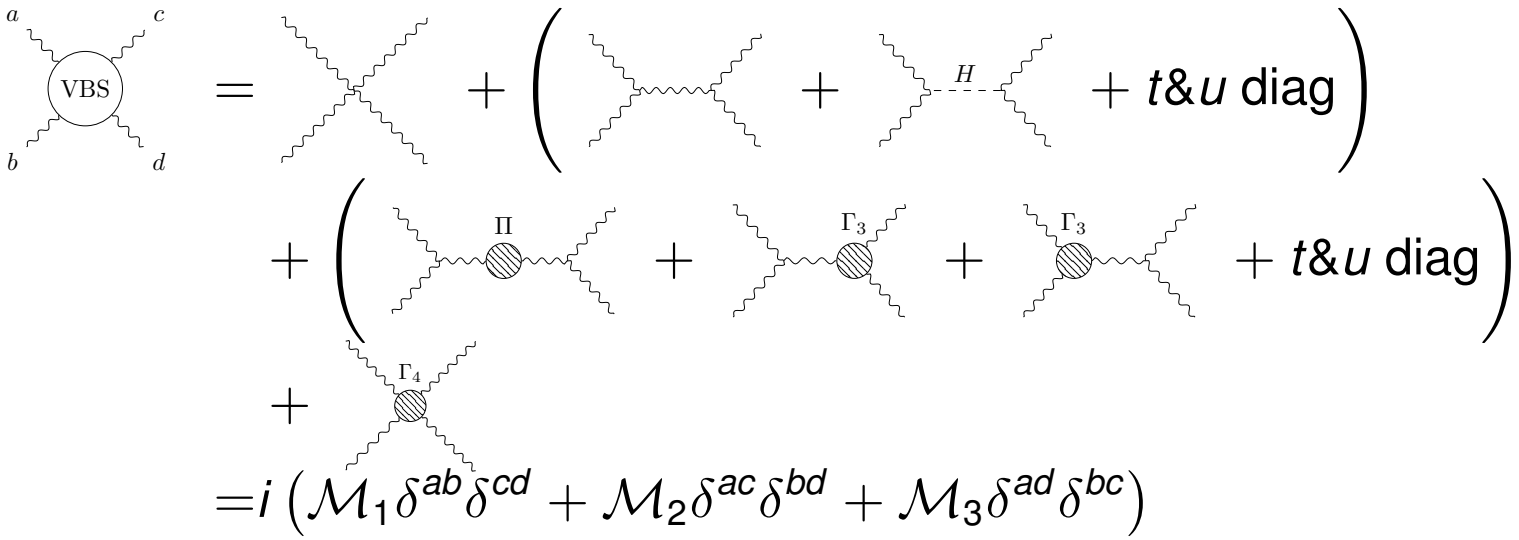

$$= i\left(\mathcal{M}_1 \delta^{ab}\delta^{cd} + \mathcal{M}_2 \delta^{ac}\delta^{bd} + \mathcal{M}_3 \delta^{ad}\delta^{bc}\right) \tag{23}$$

$\Rightarrow$ Calculate $\mathcal{M}_i$ separately and identify physical amplitudes as linear combinations

$\Rightarrow$ Calculate $\sim C_{2,F/S} T_{F/S}$ and $\sim T_{F/S}$ contributions separately for efficient reconstruction of results for various representations

- On-shell numerical calculations performed with `Fortran77` code using `LoopTools` and `CUBA` library

Partial waves (PW) and unitarity

- $2 \to 2$ helicity amplitude $\mathcal{M}_{\lambda_1\lambda_2\lambda_3\lambda_4}$ decomposed into coefficients of Wigner D-matrices

PW decomposition

$$\mathcal{M}_{\lambda_1\lambda_2\lambda_3\lambda_4}(s,\theta) = 8\pi\mathcal{N}_{fi} \sum_{j=max(|\lambda_{12}|,|\lambda_{34}|)}^{\infty} (2j+1)\mathcal{A}^j_{\lambda_1\lambda_2\lambda_3\lambda_4}(s)\, d^j_{\lambda_{12}\lambda_{34}}(\theta) \tag{24}$$

$$\mathcal{N}_{fi} = \frac{1}{\beta\sqrt{S_f S_i}} \tag{25}$$

- unitarity demands:

$$2\mathrm{Im}\left(\mathcal{A}^j_{\lambda_1\lambda_2\lambda_3\lambda_4}\right) \geq \sum_n \sum_{\lambda_1',\lambda_2'} \mathcal{A}^{j*}_{\lambda_3\lambda_4\lambda_1'\lambda_2'} \mathcal{A}^j_{\lambda_1\lambda_2\lambda_1'\lambda_2'} \tag{26}$$

Partial waves (PW) and unitarity

- Perturbative unitarity bounds for eigenvalues a^j:

$$|a^j|^2 \leq 2\,, \quad |\mathrm{Re}\,(a^j)\,| \leq 1\,, \quad 0 \leq \mathrm{Im}\,(a^j) \leq 2 \tag{27}$$

$\Rightarrow$ Visual check of perturbative unitarity through Argand diagrams

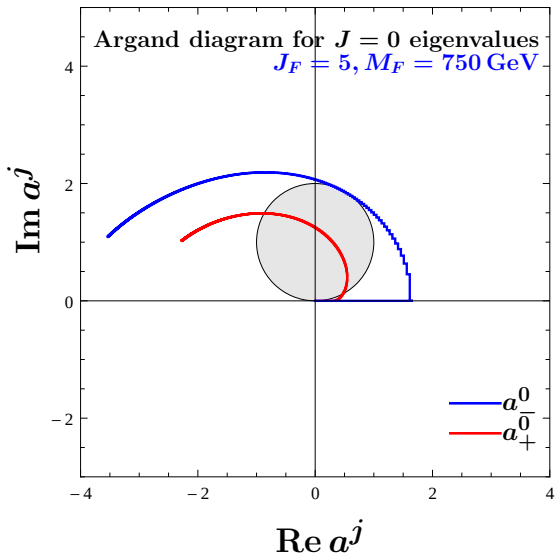

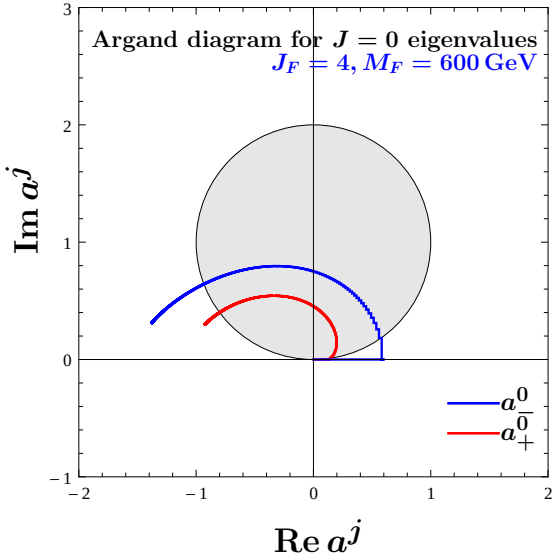

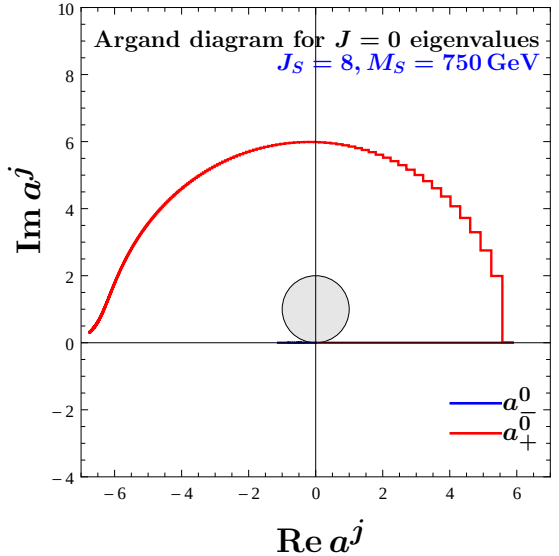

On-shell cross section

- Cross-section in center of mass frame, for scattering angles $5^\circ < \theta < 175^\circ$

$$|\mathcal{M}_{tot}|^2 = \underbrace{|\mathcal{M}_{SM}|^2 + 2\mathrm{Re}(\mathcal{M}_{SM}\mathcal{M}_{NP}^*)}_{(int)} + |\mathcal{M}_{NP}|^2$$

- Constructive interference for $WW \to ZZ$, destructive interference for $WZ \to WZ$
- Good accordance between EFT and one-loop calculation until vicinity of threshold for pair-production
- Perturbativity in the high-energy regime?

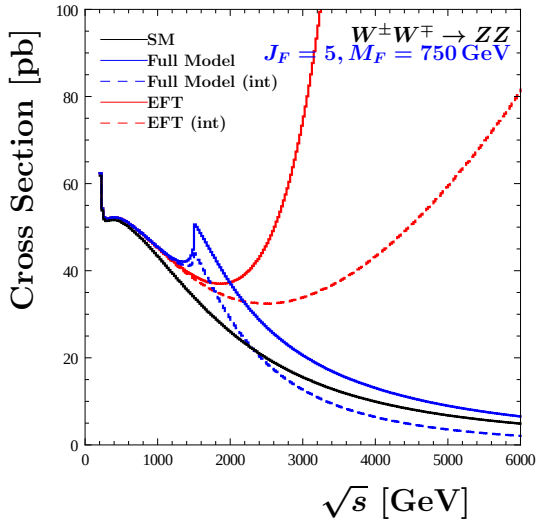

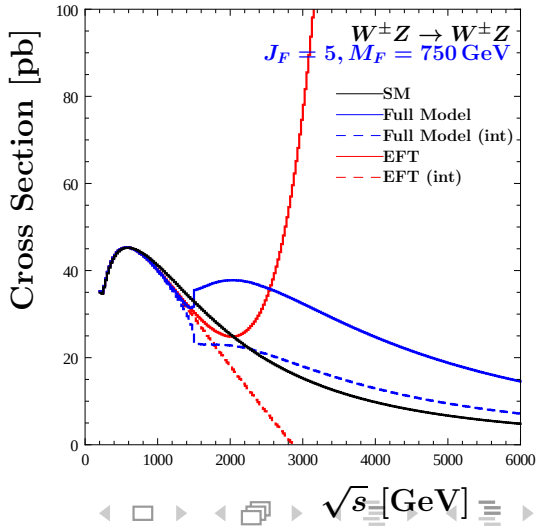

On-shell cross section

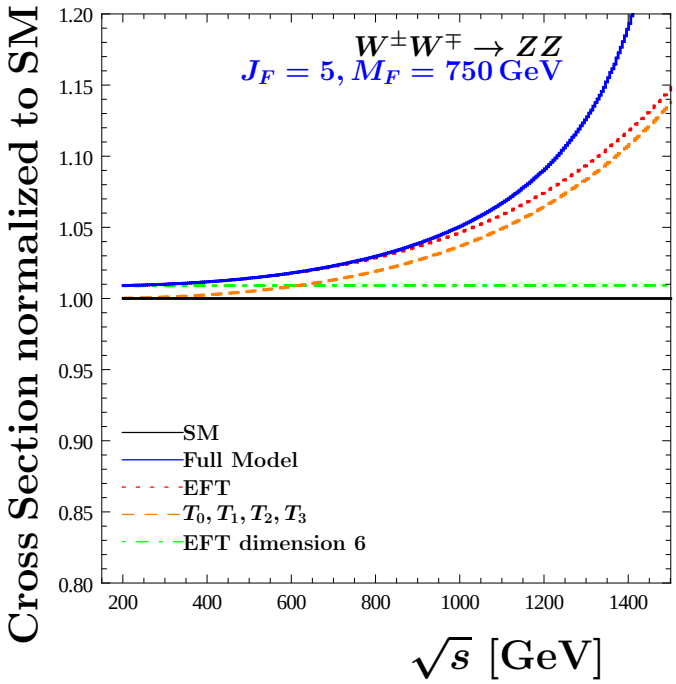

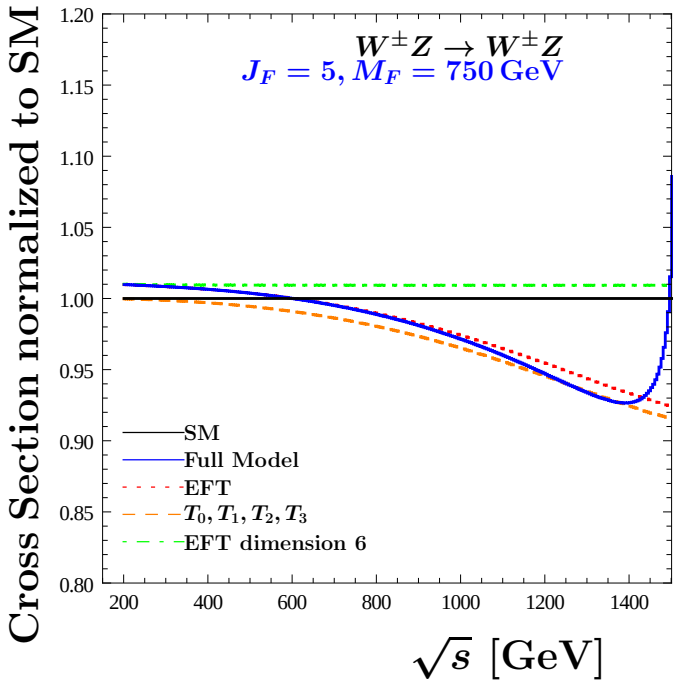

- Dimension 6 operators give relative offset to the SM, even at kinematic edge: $\frac{s}{\Lambda^2} \sim \frac{(2m_W)^2}{M_F^2}$
- Set of T-operators show relevant features of full EFT, dominant contribution for $\sqrt{s} > 600$ GeV

VBFNLO implementation

- Evaluate VBS at pp-collider (13 TeV, 35 fb^{-1}) using parton-level Monte Carlo generator `VBFNLO`
- Approximate model with dominant on-shell partial wave coefficients $\mathcal{A}^j$ up to $j = 2$, fed into pre-existing code provided by Heiko Schäfer-Siebert
- Splitting external W^3 into Z and γ channel using factors of $\sin\theta_W$, $\cos\theta_W$

Cross check and estimation for approximation error due to virtuality of momenta:

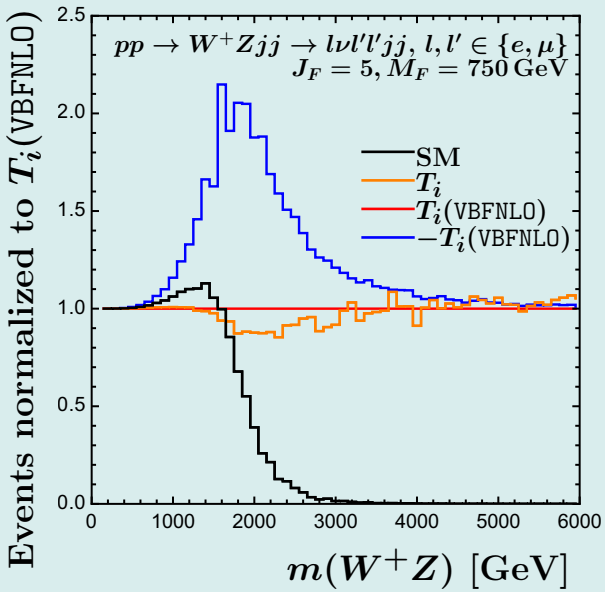

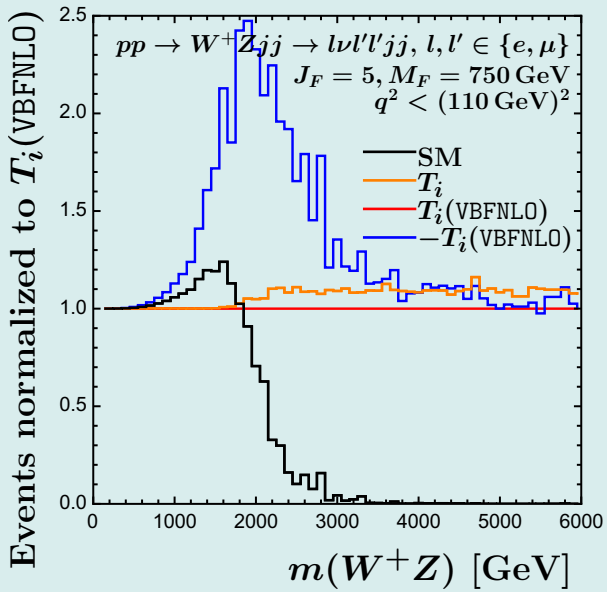

WZ production at the LHC

- Destructive interference
- Suppression in high-energy regime due to convolution with parton distribution functions
- Unphysical prediction for non-unitarized EFT in high-energy regime
- Set of T-operators and full EFT coincide
- Cancellation between T-operators for fermion model, amplification for scalar model
- EFT good approximation for limited energy range, small deviation from SM
- T_U-unitarization [arXiv:1807.02707 [hep-ph]] cannot recover high-energy behavior of full model

$\Rightarrow$ Feature of loop-induced EFT?

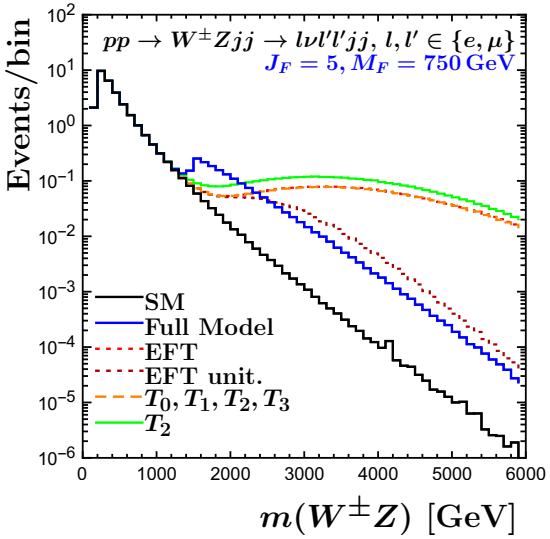

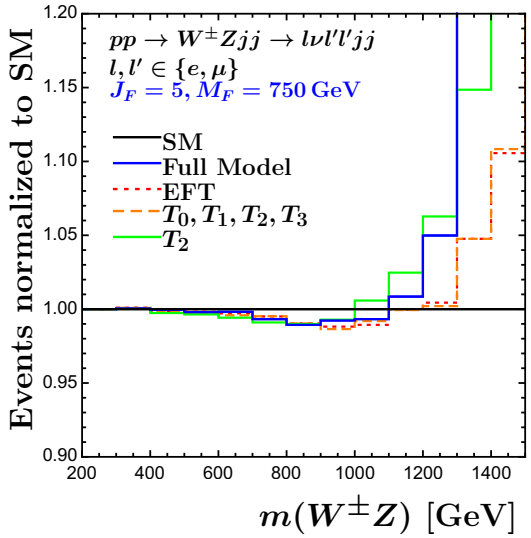

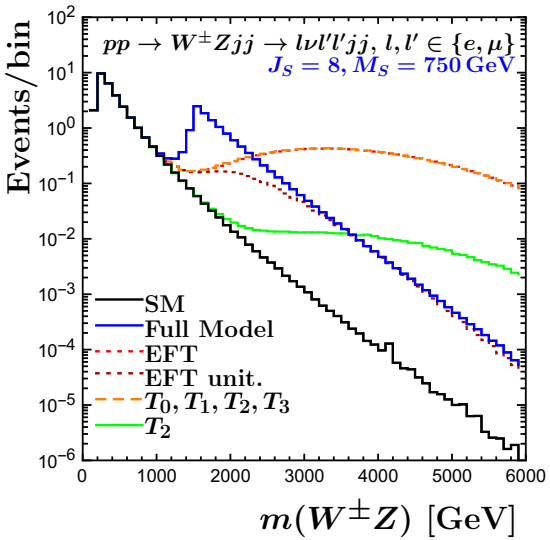

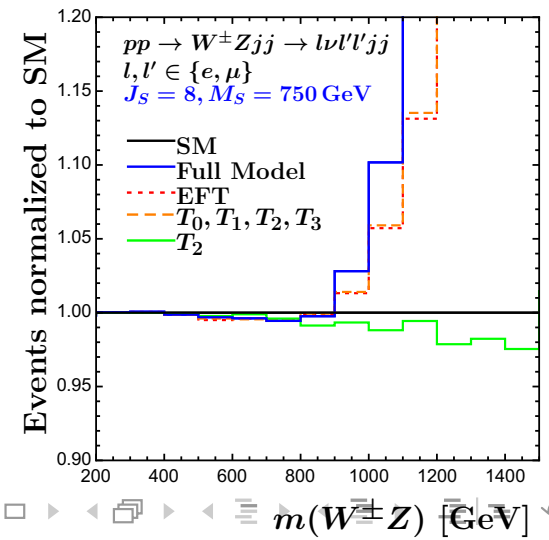

Comparison with CMS [CMS-SMP-18-001] for WZ production

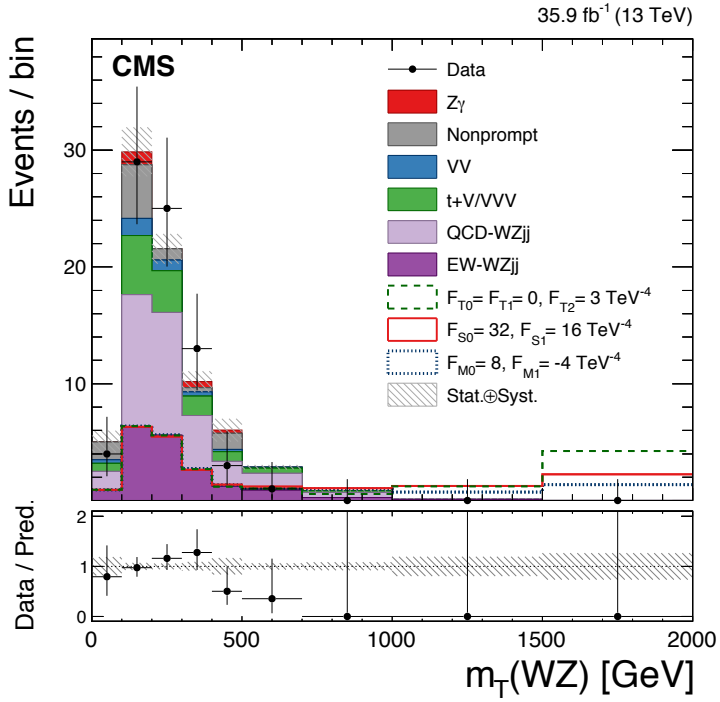

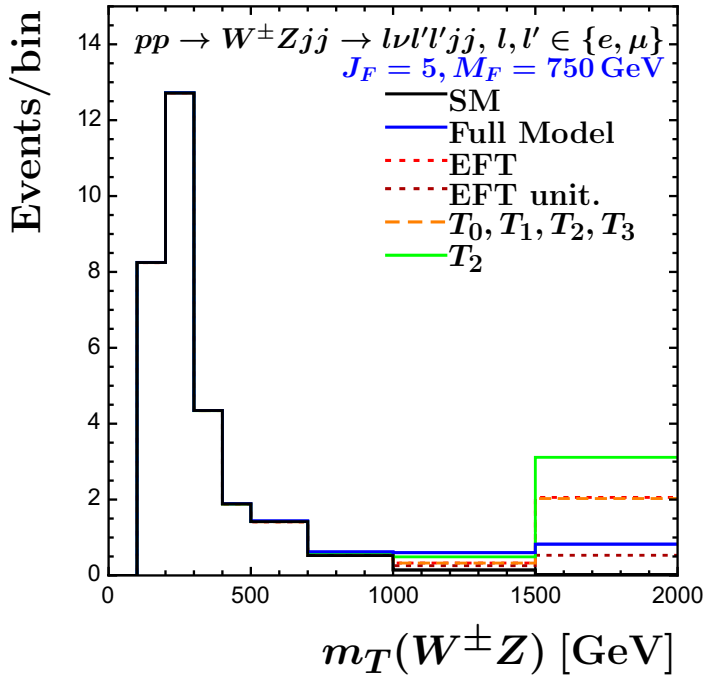

- Our SM prediction compatible with CMS EW-WZjj
- Exclusion for Wilson coefficients from last bin (> 1500 GeV), e.g. for $F_{T2} = 3\ \text{TeV}^{-4}$ (green dashed)
- Fermion model compatible within data, only pure T_2 (green solid) prediction exceeds uncertainty

Comparison with CMS [CMS-SMP-18-001] for WZ production

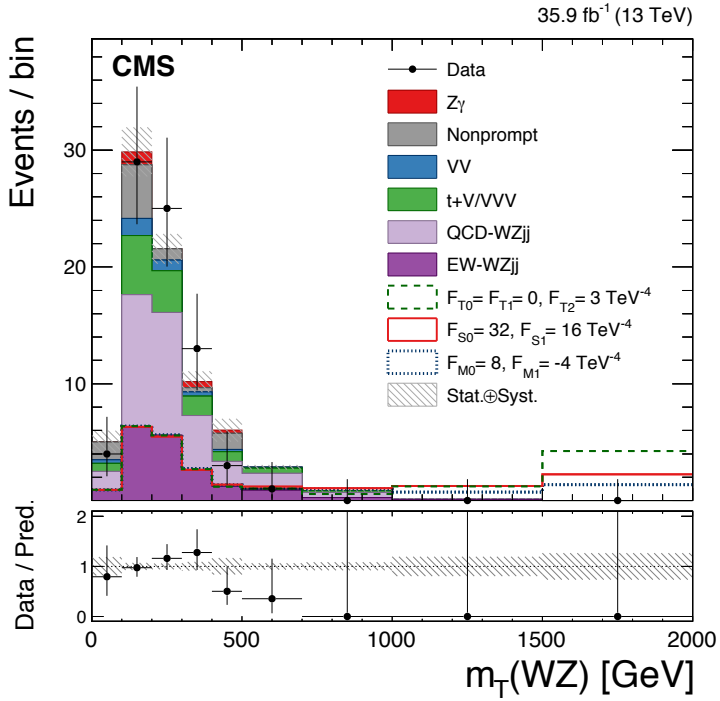

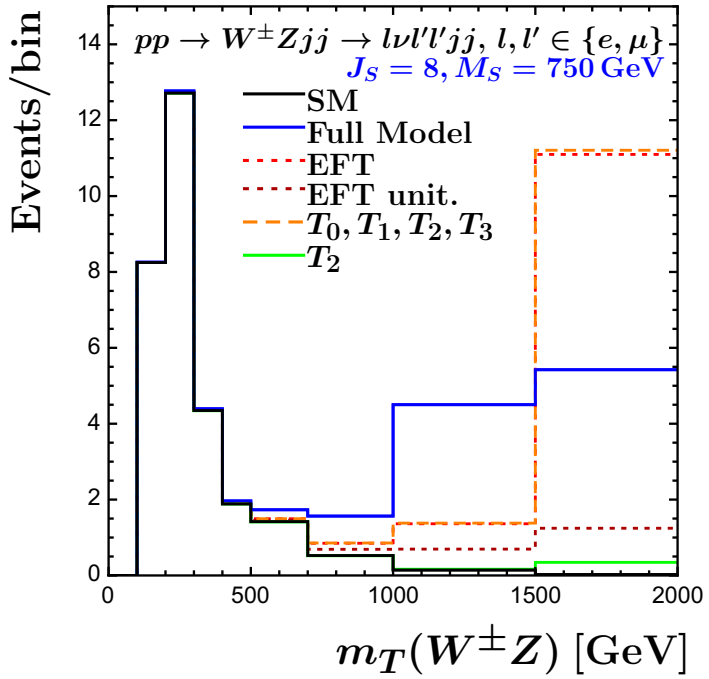

- Our SM prediction compatible with CMS EW-WZjj
- Exclusion for Wilson coefficients from last bin (> 1500 GeV), e.g. for $F_{T2} = 3\ \mathrm{TeV}^{-4}$ (green dashed)
- Fermion model compatible within data, only pure T_2 (green solid) prediction exceeds uncertainty
- Scalar model not compatible with data, but pure T_2 (green solid) prediction and unitarized EFT shows no excess

Summary and conclusion

- Constructing EFT dim 8 basis for VBS
- Model with additional $SU(2)_L$ multiplets in the $SU(2)_L$ limit of the SM
- Calculation of VBS relevant vertex corrections and Wilson coefficients
- Numerical analysis in on-shell VBS: cross section and partial waves
- Study of VBS at the LHC using approximate model implementation in `VBFNLO`
- Comparison with CMS analysis on aQGC limits

$\Rightarrow$ Model with low-energy approximation given by T-operators

$\Rightarrow$ Validity region of the EFT depends on interference with SM

$\Rightarrow$ Correlations between Wilson coefficients relevant

$\Rightarrow$ Bounds on Wilson coefficients from energy region beyond being compatible with unitarity provide limited information $\Rightarrow$ unitarization!?

Constructing basis for EFT

- All *DWWW* operators:

$$
\left.
\begin{aligned}
O_0 &= \mathrm{Tr}\big([\hat{D}_\alpha, \hat{W}^\mu{}_\nu][\hat{D}^\alpha, \hat{W}^\nu{}_\rho]\hat{W}^\rho{}_\mu\big)\\
O_{1,0} &= \mathrm{Tr}\big([\hat{D}_\alpha, \hat{W}^{\mu\nu}][\hat{D}_\beta, \hat{W}_{\mu\nu}]\hat{W}^{\alpha\beta}\big)\\
O_{1,1} &= \mathrm{Tr}\big([\hat{D}_\alpha, \hat{W}^{\mu\nu}]\hat{W}_{\mu\nu}[\hat{D}_\beta, \hat{W}^{\alpha\beta}]\big)\\
O_{2,1} &= \mathrm{Tr}\big([\hat{D}_\alpha, \hat{W}^{\mu\nu}][\hat{D}_\beta, \hat{W}^\alpha{}_\mu]\hat{W}^\beta{}_\nu\big)\\
O_{2,2} &= \mathrm{Tr}\big([\hat{D}_\beta, \hat{W}^{\mu\nu}][\hat{D}_\alpha, \hat{W}^\alpha{}_\mu]\hat{W}^\beta{}_\nu\big)\\
O_{2,3} &= \mathrm{Tr}\big([\hat{D}_\beta, \hat{W}^\alpha{}_\mu][\hat{D}_\alpha, \hat{W}^\beta{}_\nu]\hat{W}^{\mu\nu}\big)\\
O_{2,4} &= \mathrm{Tr}\big([\hat{D}_\alpha, \hat{W}^\alpha{}_\mu][\hat{D}_\beta, \hat{W}^\beta{}_\nu]\hat{W}^{\mu\nu}\big)
\end{aligned}
\right\} \Rightarrow
$$

Relations between operators

$$O_{1,1} \sim -O_{1,0}$$

$$O_{1,0} \sim 2O_{2,1}$$

$$O_{2,1} \sim O_0 - O_{2,3}$$

$$O_{2,2} \sim \tfrac{1}{2} O_{1,1}$$

$$O_{2,1} + O_{2,3} \sim O_{2,2} + O_{2,4}$$

DWWW operators used in our basis

$$O_{DWWW,0} := O_0 = \mathrm{Tr}\left([\hat{D}_\alpha, \hat{W}^\mu{}_\nu][\hat{D}^\alpha, \hat{W}^\nu{}_\rho]\hat{W}^\rho{}_\mu\right) \tag{28}$$

$$O_{DWWW,1} := O_{1,0} = \mathrm{Tr}\left([\hat{D}_\alpha, \hat{W}^{\mu\nu}][\hat{D}_\beta, \hat{W}_{\mu\nu}]\hat{W}^{\alpha\beta}\right) \tag{29}$$

Renormalization

- Only one-loop for external W-bosons $\Rightarrow$ renormalize SM $SU(2)_L$ gauge sector only
- Define $W_0^{a\,\mu} = \sqrt{Z_3} W^{a\,\mu}$ and $g_0 = Z_g g$, subscript 0 bare quantities

$$
\begin{aligned}
\mathcal{L}_{gauge} &= -\frac{1}{4} W_{0\,\mu\nu}^{a} W_0^{a\,\mu\nu} \\
&= -\frac{1}{2} W_{0\,\mu}^{a} (\partial^2 g^{\mu\nu} - \partial^\mu \partial^\nu) W_{0\,\nu}^{a} - \frac{1}{2} g_0 \epsilon^{abc} (\partial_\mu W_{0\,\nu}^{a} - \partial_\nu W_{0\,\mu}^{a}) W_0^{b\,\mu} W_0^{c\,\nu} \\
&\quad - \frac{1}{4} g_0^2 \epsilon^{abn} \epsilon^{cdn} W_{0\,\mu}^{a} W_{0\,\nu}^{b} W_0^{c\,\mu} W_0^{d\,\nu} \\
&= -Z_3 \frac{1}{2} W^{a}{}_{\mu} (\partial^2 g^{\mu\nu} - \partial^\mu \partial^\nu) W^{a}{}_{\nu} - Z_g (Z_3)^{\frac{3}{2}} \frac{1}{2} g \epsilon^{abc} (\partial_\mu W^{a}{}_{\nu} - \partial_\nu W^{a}{}_{\mu}) W^{b\,\mu} W^{c\,\nu} \\
&\quad - Z_g^2 (Z_3)^2 \frac{1}{4} g^2 \epsilon^{abn} \epsilon^{cdn} W^{a}{}_{\mu} W^{b}{}_{\nu} W^{c\,\mu} W^{d\,\nu}
\end{aligned}
\tag{30}
$$

- Expanding $Z_3 = 1 + \delta_3$, $Z_g = 1 + \delta_g$ gives the necessary counter term vertices

Renormalization

- W propagator

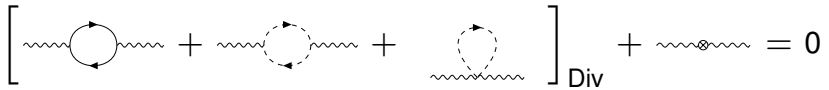

$$\delta_3 = -g^2 \Delta_\epsilon \left(n_F \frac{T_F}{12\pi^2} + n_S \frac{T_S}{48\pi^2} \right) \tag{32}$$

- $3W$ vertex

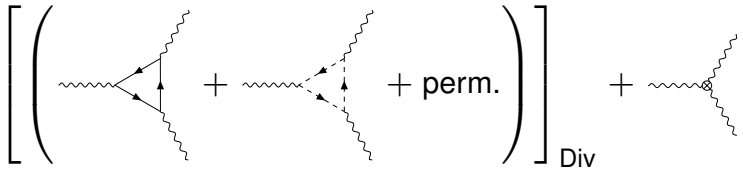

$$\Rightarrow \left(\delta_g + \frac{3}{2}\delta_3 \right) = -g^2 \Delta_\epsilon \left(n_F \frac{T_F}{12\pi^2} + n_S \frac{T_S}{48\pi^2} \right) \tag{34}$$

$$\Leftrightarrow \delta_g = \frac{g^2}{2} \Delta_\epsilon \left(n_F \frac{T_F}{12\pi^2} + n_S \frac{T_S}{48\pi^2} \right) \tag{35}$$

- $4W$ vertex

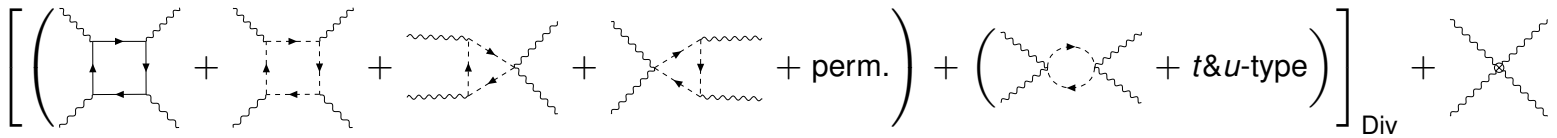

$$\Rightarrow 2\left(\delta_g + \delta_3\right) = \delta_3 = -g^2 \Delta_\epsilon \left(n_F \frac{T_F}{12\pi^2} + n_S \frac{T_S}{48\pi^2} \right) \tag{37}$$

Matching of Wilson Coefficients

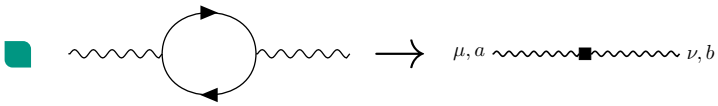

$$f_{WW,F} = -g^2 \frac{T_F}{24\pi^2}\left(\Delta_\epsilon - \log\left(\frac{M_F^2}{\mu^2}\right)\right) \qquad f_{WW,S} = -g^2 \frac{T_S}{96\pi^2}\left(\Delta_\epsilon - \log\left(\frac{M_S^2}{\mu^2}\right)\right) \tag{38}$$

$$\frac{f_{DW,F}}{\Lambda^2} = -g^2 \frac{T_F}{120\pi^2 M_F^2} \qquad \frac{f_{DW,S}}{\Lambda^2} = -g^2 \frac{T_S}{960\pi^2 M_S^2} \tag{39}$$

$$\frac{f_{D2W,F}}{\Lambda^4} = -g^2 \frac{T_F}{1120\pi^2 M_F^4} \qquad \frac{f_{D2W,S}}{\Lambda^4} = -g^2 \frac{T_S}{13440\pi^2 M_S^4} \tag{40}$$

Matching of Wilson Coefficients

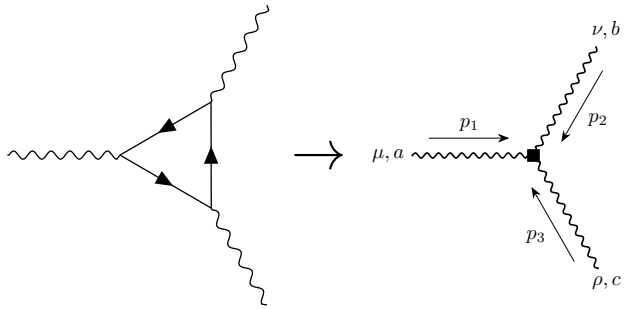

$$\frac{f_{WWW,F}}{\Lambda^2} = i\,g^3\,\frac{13\,T_F}{360\pi^2 M_F^2}$$

$$\frac{f_{DWWW,0,F}}{\Lambda^4} = i\,g^3\,\frac{2\,T_F}{105\pi^2 M_F^4}$$

$$\frac{f_{DWWW,1,F}}{\Lambda^4} = i\,g^3\,\frac{T_F}{630\pi^2 M_F^4}$$

$$\frac{f_{WWW,S}}{\Lambda^2} = i\,g^3\,\frac{T_S}{360\pi^2 M_S^2} \tag{41}$$

$$\frac{f_{DWWW,0,S}}{\Lambda^4} = i\,g^3\,\frac{T_S}{1120\pi^2 M_S^4} \tag{42}$$

$$\frac{f_{DWWW,1,S}}{\Lambda^4} = i\,g^3\,\frac{T_S}{4032\pi^2 M_S^4} \tag{43}$$

Matching of Wilson Coefficients

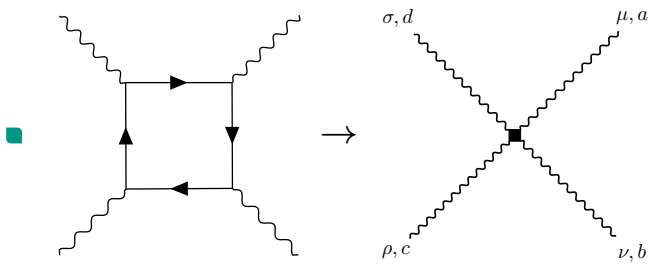

$$\frac{f_{T,0,F}}{\Lambda^4} = g^4 \frac{T_F}{10080\pi^2 M_F^4}\left(-14C_{2,F}+1\right)$$

$$\frac{f_{T,1,F}}{\Lambda^4} = g^4 \frac{T_F}{10080\pi^2 M_F^4}\left(-28C_{2,F}+13\right)$$

$$\frac{f_{T,2,F}}{\Lambda^4} = g^4 \frac{T_F}{25200\pi^2 M_F^4}\left(196C_{2,F}-397\right)$$

$$\frac{f_{T,3,F}}{\Lambda^4} = g^4 \frac{T_F}{25200\pi^2 M_F^4}\left(98C_{2,F}+299\right)$$

$$\frac{f_{T,0,S}}{\Lambda^4} = g^4 \frac{T_S}{40320\pi^2 M_S^4}\left(7C_{2,S}-2\right) \quad (44)$$

$$\frac{f_{T,1,S}}{\Lambda^4} = g^4 \frac{T_S}{40320\pi^2 M_S^4}\left(14C_{2,S}-5\right) \quad (45)$$

$$\frac{f_{T,2,S}}{\Lambda^4} = g^4 \frac{T_S}{50400\pi^2 M_S^4}\left(14C_{2,S}-23\right) \quad (46)$$

$$\frac{f_{T,3,S}}{\Lambda^4} = g^4 \frac{T_S}{50400\pi^2 M_S^4}\left(7C_{2,S}+16\right) \quad (47)$$

Definitions for on-shell VBS

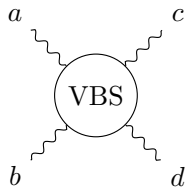

$$= i\left(\mathcal{M}_1\delta^{ab}\delta^{cd} + \mathcal{M}_2\delta^{ac}\delta^{bd} + \mathcal{M}_3\delta^{ad}\delta^{bc}\right) \tag{48}$$

Scattering of physical states

$$\begin{aligned}
\mathcal{M}\left(W^\pm W^\mp \to ZZ\right) &= \mathcal{M}_1 = \mathcal{M}\left(ZZ \to W^\pm W^\mp\right)\\
\mathcal{M}\left(W^\pm Z \to W^\pm Z\right) &= \mathcal{M}_2\\
\mathcal{M}\left(W^\pm Z \to Z W^\pm\right) &= \mathcal{M}_3\\
\mathcal{M}\left(W^\pm W^\mp \to W^\pm W^\mp\right) &= \mathcal{M}_1 + \mathcal{M}_2\\
\mathcal{M}\left(W^\pm W^\mp \to W^\mp W^\pm\right) &= \mathcal{M}_1 + \mathcal{M}_3\\
\mathcal{M}\left(W^\pm W^\pm \to W^\pm W^\pm\right) &= \mathcal{M}_2 + \mathcal{M}_3\\
\mathcal{M}\left(ZZ \to ZZ\right) &= \mathcal{M}_1 + \mathcal{M}_2 + \mathcal{M}_3
\end{aligned} \tag{49}$$

Kinematics on-shell VBS

- Momenta COM-frame:

$$\begin{aligned} p_1 &= \frac{\sqrt{s}}{2}(1,0,0,\beta) & q_1 &= \frac{\sqrt{s}}{2}(1,\beta\sin(\theta),0,\beta\cos(\theta)) \\ p_2 &= \frac{\sqrt{s}}{2}(1,0,0,-\beta) & q_2 &= \frac{\sqrt{s}}{2}(1,-\beta\sin(\theta),0,-\beta\cos(\theta)) \end{aligned} \tag{50}$$

- Mandelstam variables:

$$s = (p_1+p_2)^2 \tag{51}$$

$$t = (p_1-q_1)^2 = -\frac{\sqrt{s}\beta^2}{2}(1-\cos(\theta)) \tag{52}$$

$$u = (p_1-q_2)^2 = -\frac{\sqrt{s}\beta^2}{2}(1+\cos(\theta)) \tag{53}$$

- Polarization vectors[1]:

$$\begin{aligned} \epsilon_\pm(p_1) &= -\frac{1}{\sqrt{2}}(0,1,\pm i,0) & \epsilon_0(p_1) &= \frac{\sqrt{s}}{2m_W}(\beta,0,0,1) \\ \epsilon_\pm(p_2) &= -\frac{1}{\sqrt{2}}(0,1,\mp i,0) & \epsilon_0(p_2) &= \frac{\sqrt{s}}{2m_W}(\beta,0,0,-1) \\ \epsilon^*_\pm(q_1) &= -\frac{1}{\sqrt{2}}(0,\cos(\theta),-\sin(\theta)\mp i,0) & \epsilon^*_0(q_1) &= \frac{\sqrt{s}}{2m_W}(\beta,\sin(\theta),0,\sin(\theta)) \\ \epsilon^*_\pm(q_2) &= -\frac{1}{\sqrt{2}}(0,\cos(\theta),-\sin(\theta)\pm i,0) & \epsilon^*_0(q_2) &= \frac{\sqrt{s}}{2m_W}(\beta,-\sin(\theta),0,-\cos(\theta)) \end{aligned} \tag{54}$$

[1] Using definitions from: [Hagiwara, K. and Zeppenfeld, D. (1989); https://doi.org/10.1016/0550-3213(89)90397-0]

EFT Power Counting

- Estimate suppression/enhancement of various contributions in expected validity region of EFT from kinematic edge $\sqrt{s} \sim 2m_W$ to NP scale $\sqrt{s} \sim M_F = 750\,\text{GeV}$

$\Rightarrow$ Loop-factor $\frac{g^2}{16\pi^2}$ for one-loop matching and EW corrections

$\Rightarrow$ Energy behavior of EFT vertices $\sim \frac{s}{\Lambda^2}$ for dimension 6 and $\sim \left(\frac{s}{\Lambda^2}\right)^2$ for dimension 8

$\Rightarrow$ Leading behavior of representation factors of EFT vertices for $J_F = 5$

$\mathcal{M}_i$	$2\text{Re}\left(\mathcal{M}_{SM}\mathcal{M}_i\right)$	$\frac{s}{\Lambda^2} \to [\frac{(2m_W)^2}{M_F^2}, 1]$	$\lvert\mathcal{M}_i\rvert^2$	$\frac{s}{\Lambda^2} \to [\frac{(2m_W)^2}{M_F^2}, 1]$
$\mathcal{M}_{f_{WWW}}$	$\frac{g^2}{16\pi^2}\frac{s}{\Lambda^2}J_R^3$	$[0.01616, 0.34481]$	$\left(\frac{g^2}{16\pi^2}\right)^2\frac{s^2}{\Lambda^4}J_R^6$	$[0.00026, 0.11889]$
$\mathcal{M}_{f_{T_i}}$	$\frac{g^2}{16\pi^2}\frac{s^2}{\Lambda^4}J_R^5$	$[0.01893, 8.62022]$	$\left(\frac{g^2}{16\pi^2}\right)^2\frac{s^4}{\Lambda^8}J_R^{10}$	$[0.00036, 74.3081]$
$\mathcal{M}_{f^2_{WWW}}$	$\left(\frac{g^2}{16\pi^2}\right)^2\frac{s^2}{\Lambda^4}J_R^6$	$[0.00026, 0.11889]$	$\left(\frac{g^2}{16\pi^2}\right)^4\frac{s^4}{\Lambda^8}J_R^{12}$	$[6.8\cdot10^{-8}, 0.01414]$
$\mathcal{M}_{SM}^{NLO}$	$\frac{g^2}{16\pi^2}$	$[0.00276, 0.00276]$	$\left(\frac{g^2}{16\pi^2}\right)^2$	$[7.6\cdot10^{-6}, 7.6\cdot10^{-6}]$
$\mathcal{M}_{f_{WWW}}^{NLO}$	$\left(\frac{g^2}{16\pi^2}\right)^2\frac{s}{\Lambda^2}J_R^3$	$[0.00004, 0.00095]$	$\left(\frac{g^2}{16\pi^2}\right)^4\frac{s^2}{\Lambda^4}J_R^6$	$[2.0\cdot10^{-9}, 9.0\cdot10^{-7}]$
$\mathcal{M}_{f_{T_i}}^{NLO}$	$\left(\frac{g^2}{16\pi^2}\right)^2\frac{s^2}{\Lambda^4}J_R^5$	$[0.00005, 0.02378]$	$\left(\frac{g^2}{16\pi^2}\right)^4\frac{s^4}{\Lambda^8}J_R^{10}$	$[2.7\cdot10^{-9}, 0.00057]$

Diagonalization of partial wave coefficients

- Diagonalize helicity space

$$\begin{aligned}
&\begin{pmatrix} \frac{1}{\sqrt{2}} & \frac{1}{\sqrt{2}} \\ \frac{1}{\sqrt{2}} & -\frac{1}{\sqrt{2}} \end{pmatrix} \cdot \begin{pmatrix} \mathcal{A}^0_{1111} & \mathcal{A}^0_{11\text{-}1\text{-}1} \\ \mathcal{A}^0_{\text{-}1\text{-}111} & \mathcal{A}^0_{\text{-}1\text{-}1\text{-}1\text{-}1} \end{pmatrix} \cdot \begin{pmatrix} \frac{1}{\sqrt{2}} & \frac{1}{\sqrt{2}} \\ \frac{1}{\sqrt{2}} & -\frac{1}{\sqrt{2}} \end{pmatrix} \\
&= \begin{pmatrix} \mathcal{A}^0_{1111} + \mathcal{A}^0_{11\text{-}1\text{-}1} & 0 \\ 0 & \mathcal{A}^0_{1111} - \mathcal{A}^0_{11\text{-}1\text{-}1} \end{pmatrix} \\
&=: \begin{pmatrix} \mathcal{A}^0_+ & 0 \\ 0 & \mathcal{A}^0_- \end{pmatrix}
\end{aligned} \tag{55}$$

- Diagonalize isospin space

$$\begin{pmatrix}
A(W^\pm W^\pm \to W^\pm W^\pm) & 0 & 0 & 0 & 0 & 0 \\
0 & \frac{A(W^\pm Z \to W^\pm Z)}{2} & \frac{A(W^\pm Z \to Z W^\pm)}{2} & 0 & 0 & 0 \\
0 & \frac{A(Z W^\pm \to W^\pm Z)}{2} & \frac{A(Z W^\pm \to Z W^\pm)}{2} & 0 & 0 & 0 \\
0 & 0 & 0 & \frac{A(W^+ W^- \to W^+ W^-)}{2} & \frac{A(W^+ W^- \to ZZ)}{\sqrt{2}} & \frac{A(W^+ W^- \to W^- W^+)}{2} \\
0 & 0 & 0 & \frac{A(ZZ \to W^+ W^-)}{\sqrt{2}} & A(ZZ \to ZZ) & \frac{A(ZZ \to W^- W^+)}{\sqrt{2}} \\
0 & 0 & 0 & \frac{A(W^- W^+ \to W^+ W^-)}{2} & \frac{A(W^- W^+ \to ZZ)}{\sqrt{2}} & \frac{A(W^- W^+ \to W^- W^+)}{2}
\end{pmatrix} \tag{56}$$

Dominant partial wave coefficients ($J_F = 5, M_F = 750\,\text{GeV}$)

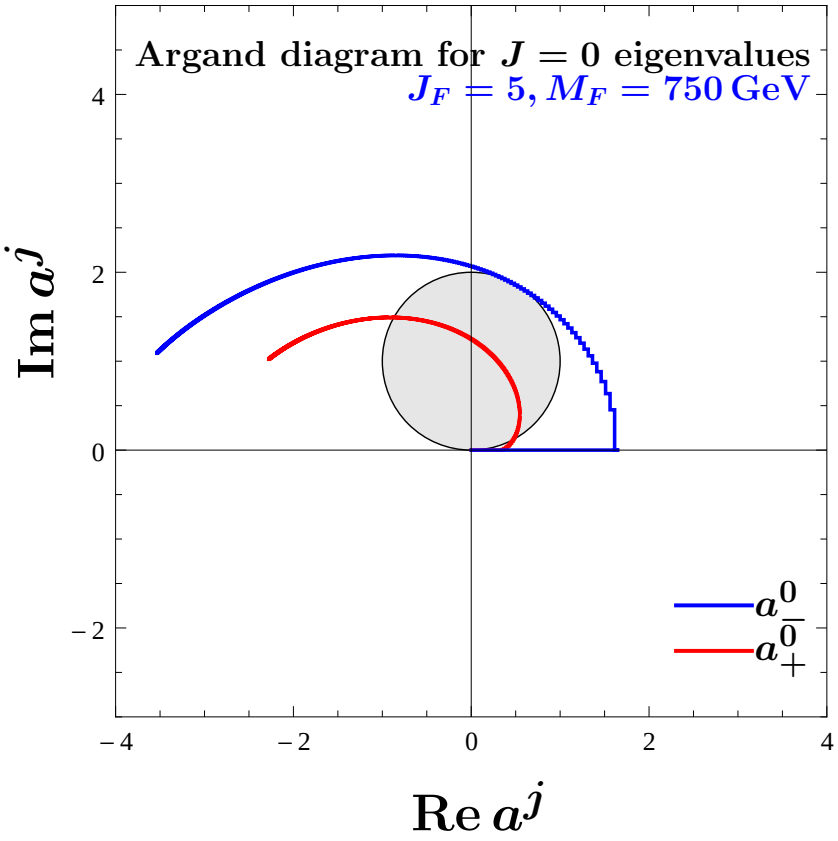

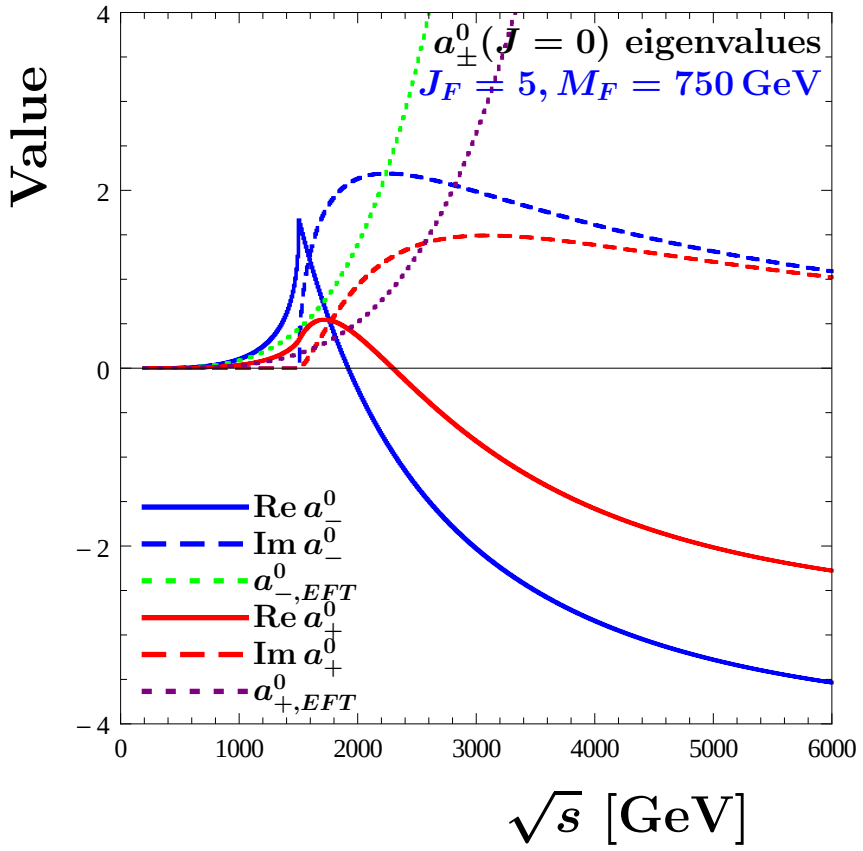

On-shell cross section ($J_F = 5, M_F = 750\,\text{GeV}$)

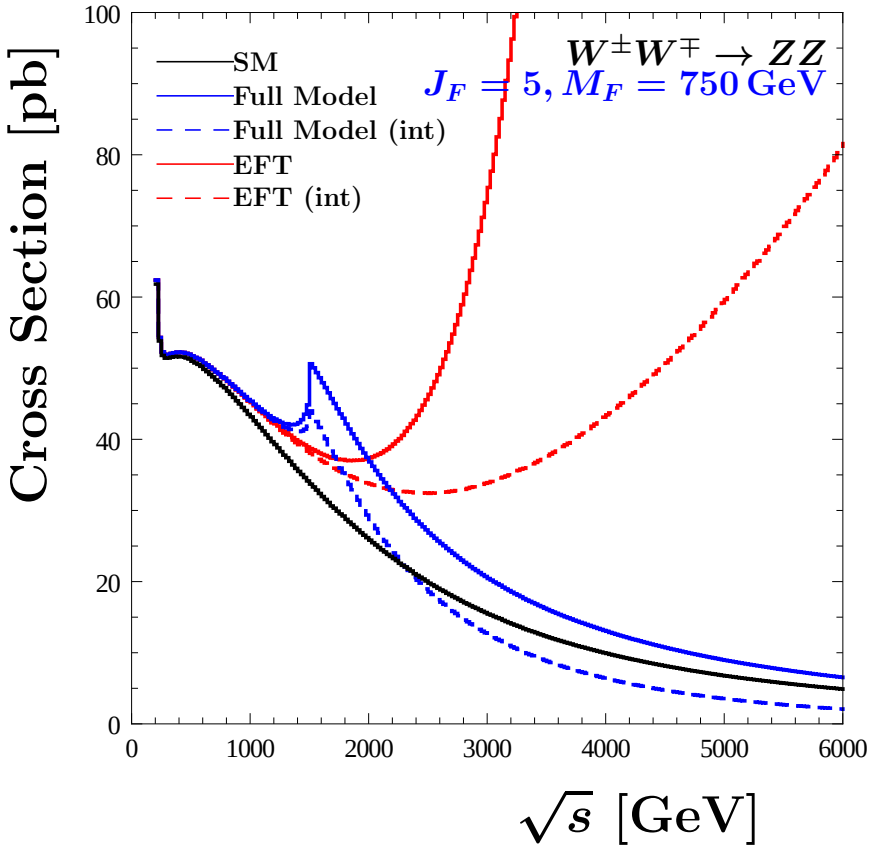

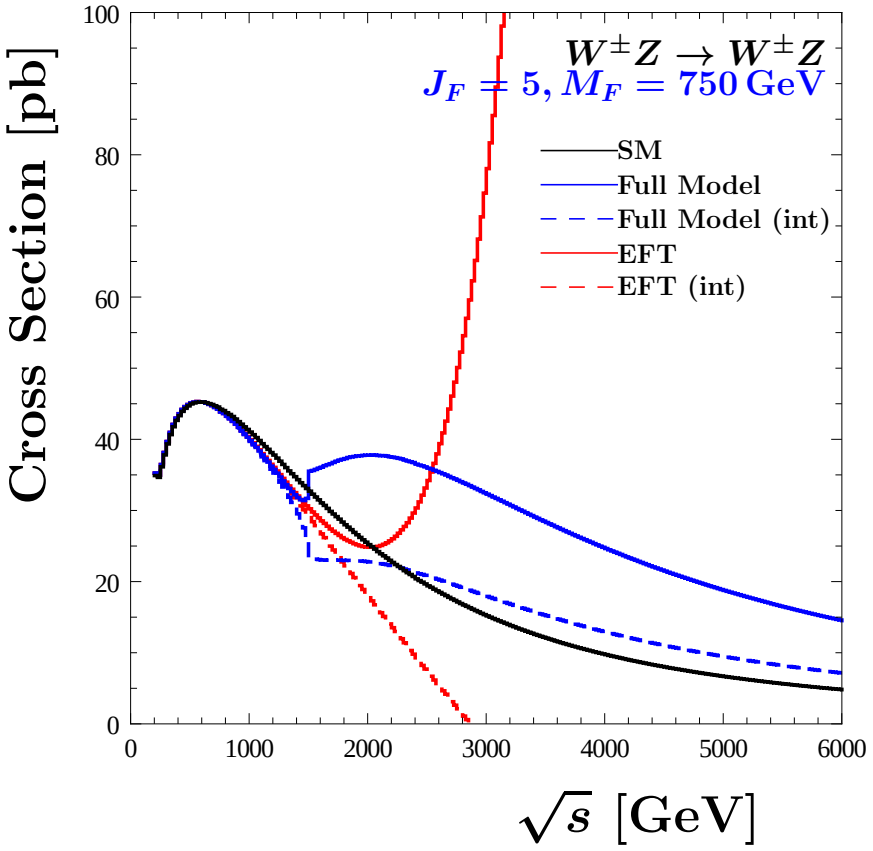

Dominant partial wave coefficients ($J_F = 4, M_F = 600\,\text{GeV}$)

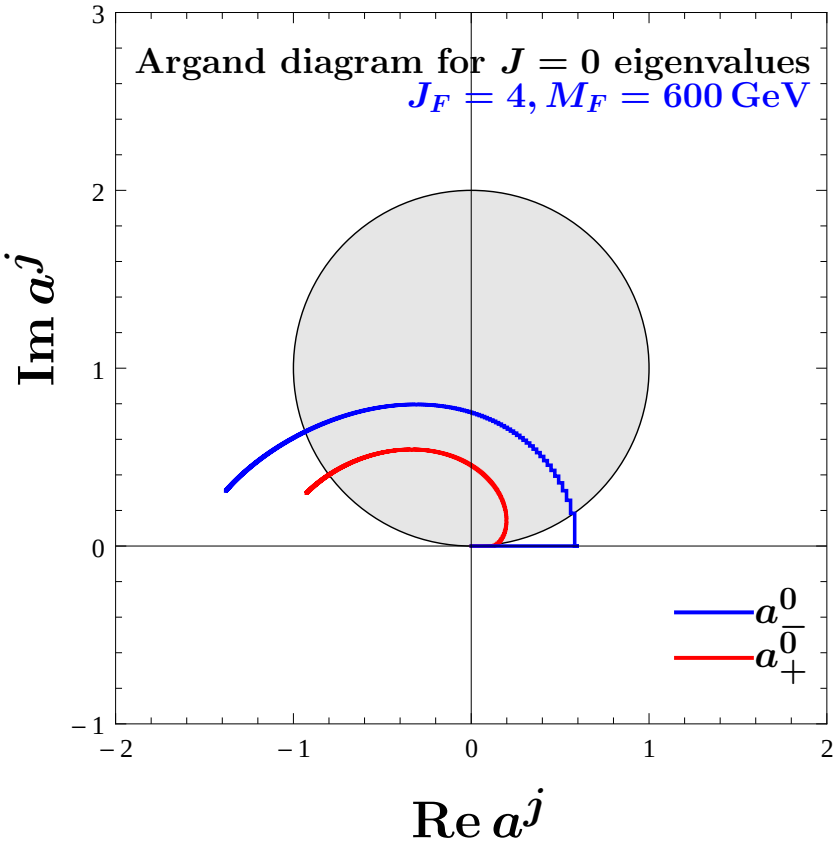

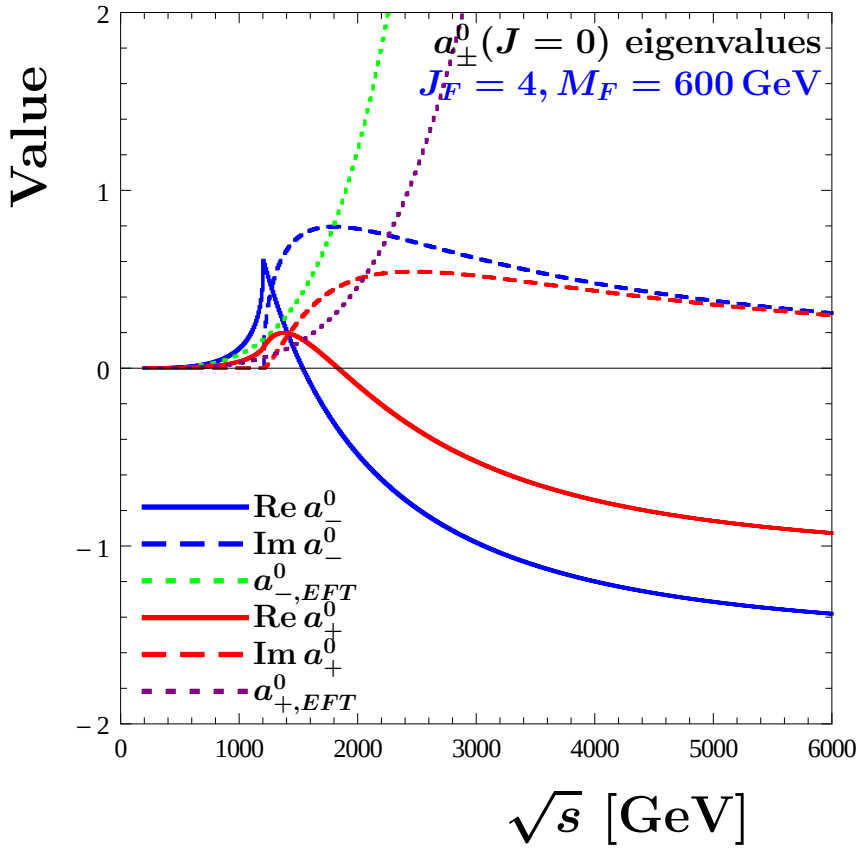

On-shell cross section ($J_F = 4, M_F = 600\,\text{GeV}$)

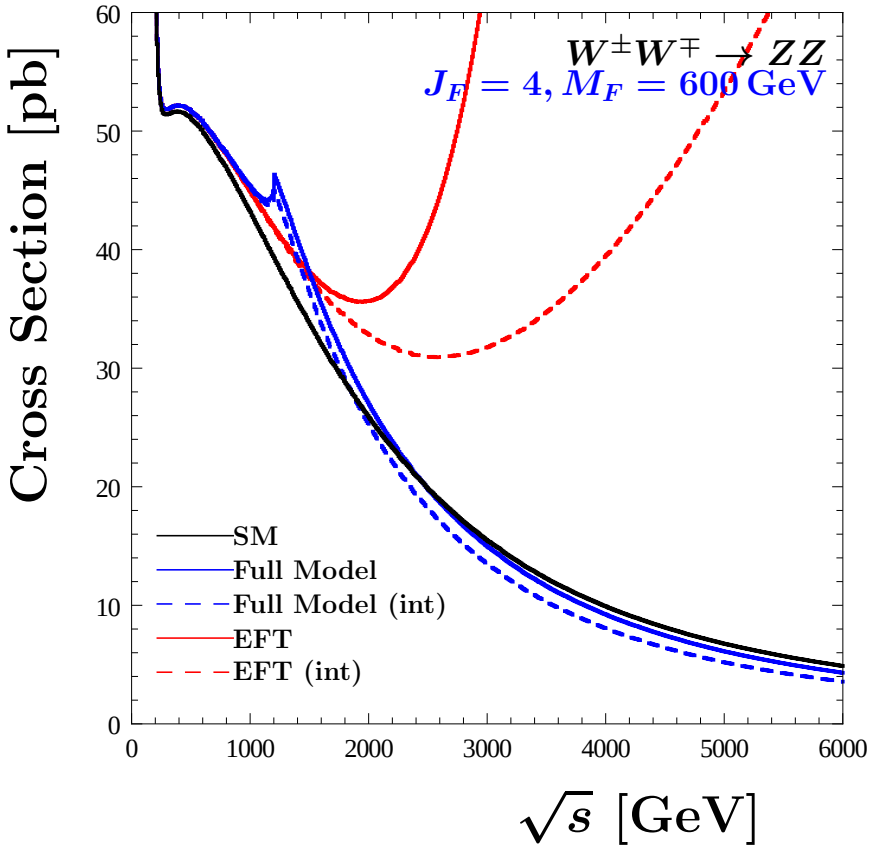

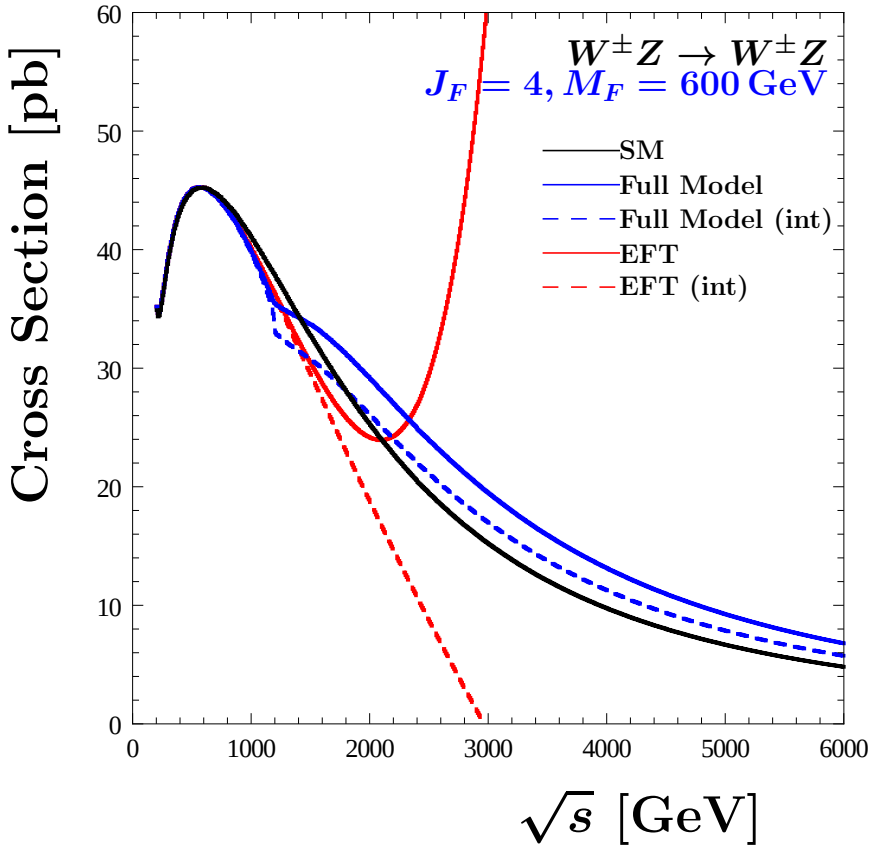

VBFNLO implementation

- Cutflow *WZ* production:

$$
\begin{aligned}
p_T^{l'}, p_T^{l} &> 20\,\text{GeV}\,, & |\eta^{e}| &< 2.5\,, & |\eta^{\mu}| &< 2.4\,,\\
|m_{ll} - m_Z| &< 15\,\text{GeV}\,, & m_{3l} &> 100\,\text{GeV}\,, & p_T^{\text{miss}} &> 30\,\text{GeV}\,,\\
|\eta^{j}| &< 4.7\,, & p_T^{j} &> 50\,\text{GeV}\,, & |\Delta R(j,l)| &> 0.4\\
m_{jj} &> 500\,\text{GeV}\,, & |\Delta\eta_{jj}| &> 2.5\,, & |\eta^{3l} - \frac{\eta^{j_1} + \eta^{j_2}}{2}| &< 2.5\,.
\end{aligned}
\tag{57}
$$

- Cutflow *ZZ* production:

$$
\begin{aligned}
p_T^{l'}, p_T^{l} &> 20\,\text{GeV}\,, & |\eta^{e}| &< 2.5\,, & |\eta^{\mu}| &< 2.4\,,\\
40\,\text{GeV} < m_{ll}, m_{l'l'} &< 120\,\text{GeV}\,, & |\eta^{j}| &< 4.7\,, & p_T^{j} &> 30\,\text{GeV}\,,\\
|\Delta R(j,l)| &> 0.3\,, & m_{jj} &> 400\,\text{GeV}\,, & |\Delta\eta_{jj}| &> 2.4\,.
\end{aligned}
\tag{58}
$$

Comparison with CMS [CMS-SMP-18-001] for WZ scattering

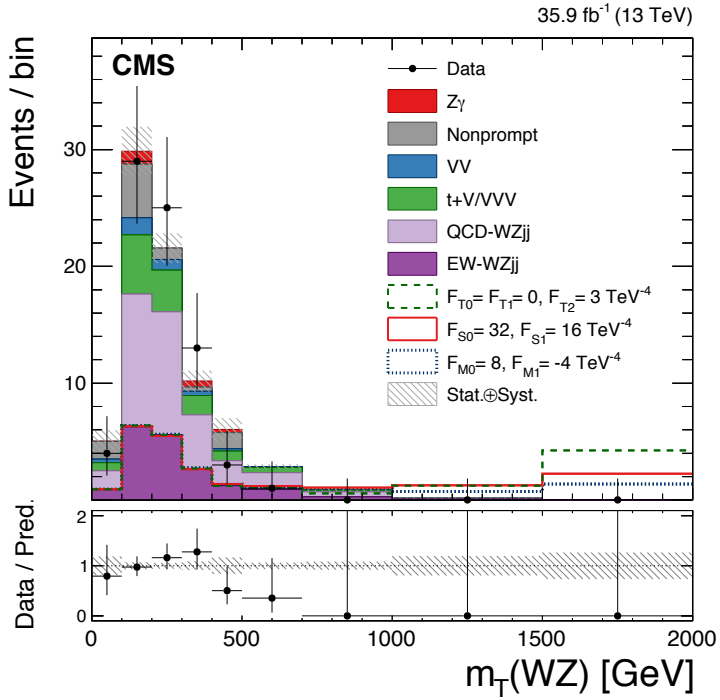

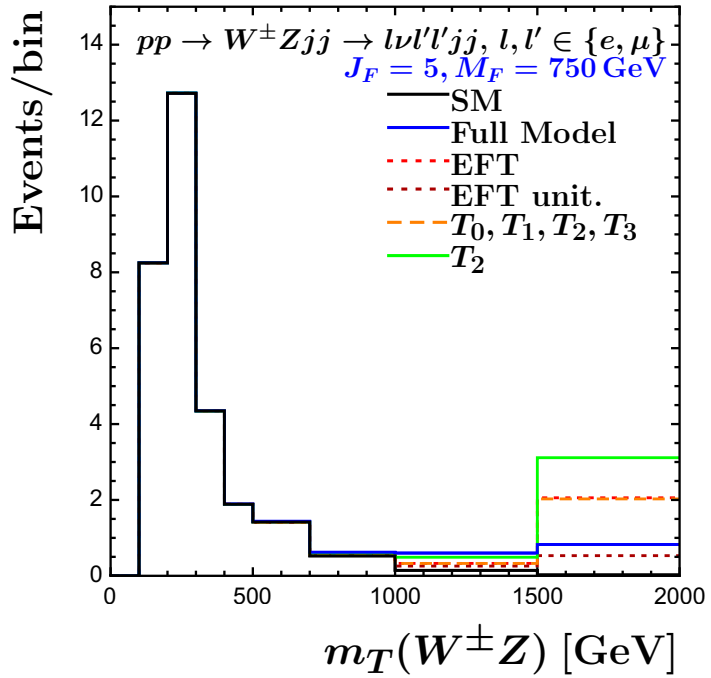

Comparison with CMS [CMS-SMP-18-001] for WZ scattering

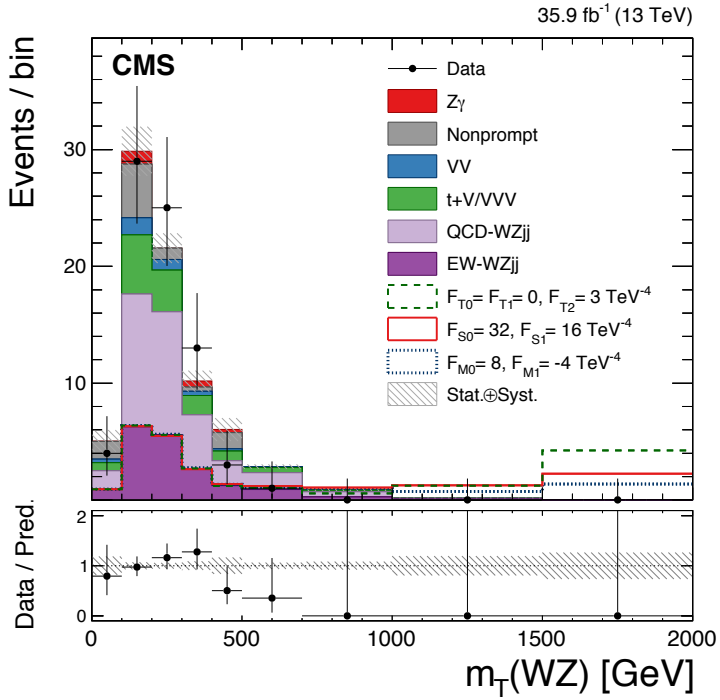

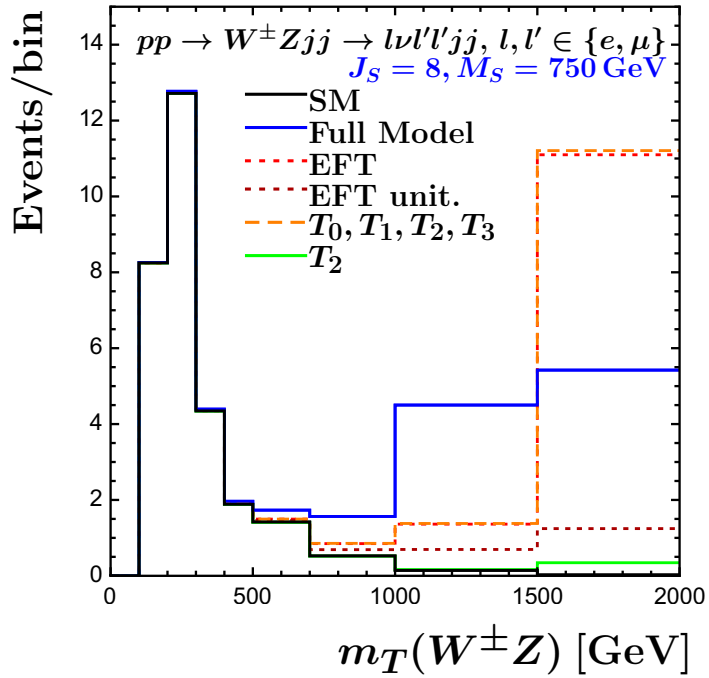

Comparison with CMS [CMS-SMP-17-006] for ZZ scattering

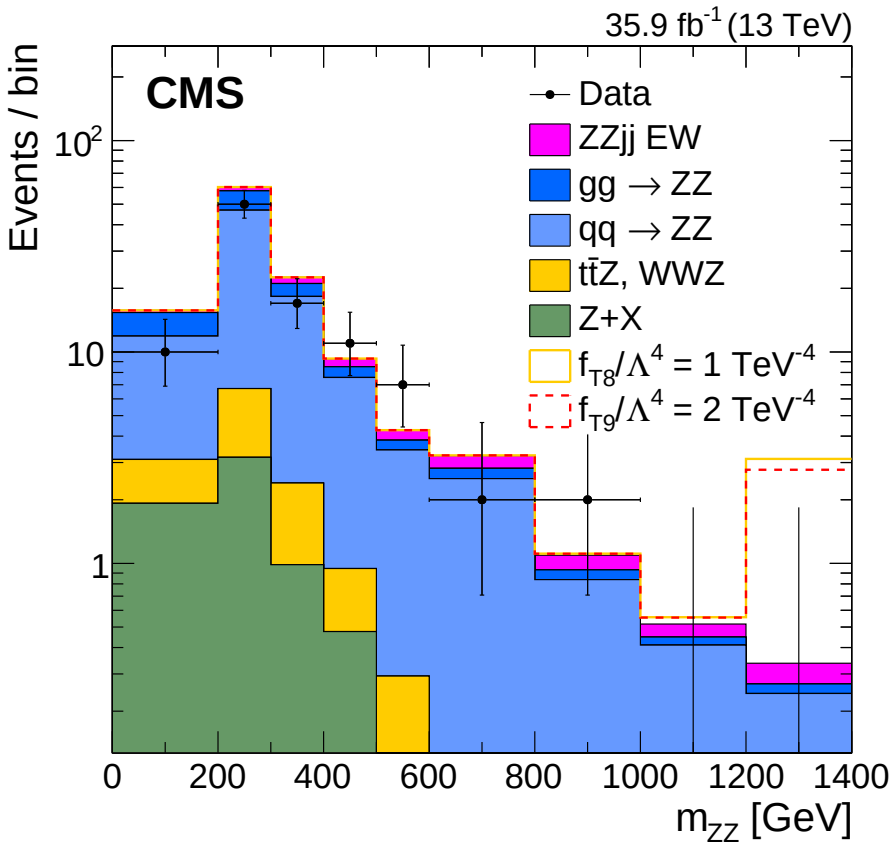

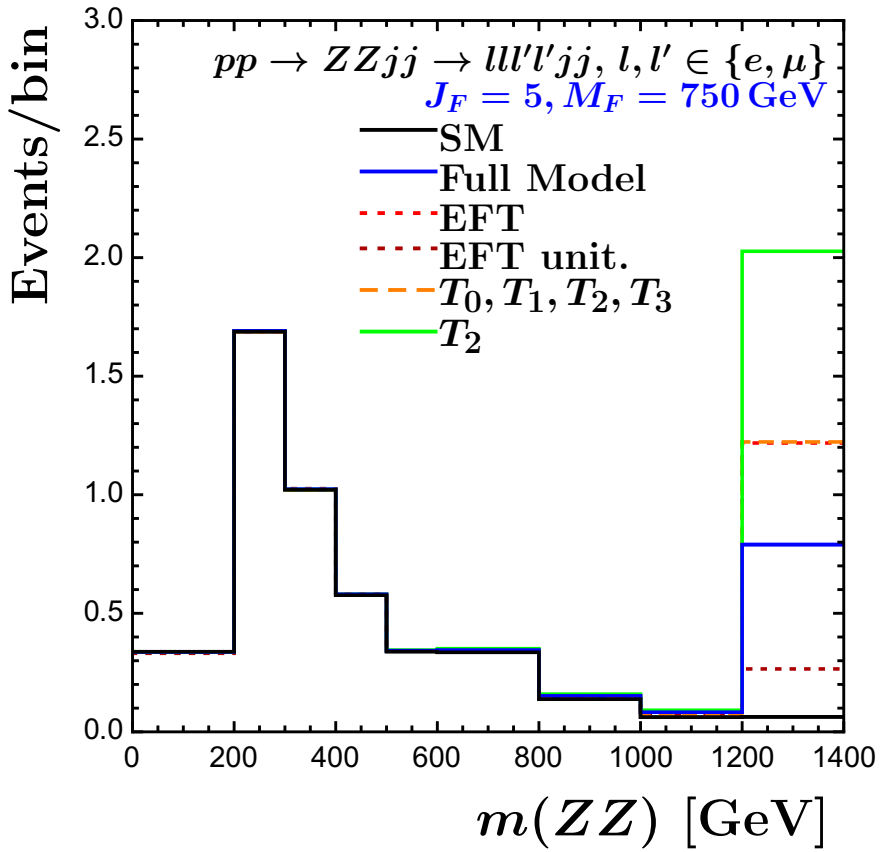

Comparison with CMS [CMS-SMP-17-006] for ZZ scattering